IMAGE-BASED CILIARY BEATING FREQUENCY ESTIMATION FOR THERAPEUTIC ASSESSMENT ON DEFECTIVE MUCOCILIARY CLEARANCE DISEASES

Fan Zhang[1], Weidong Cai[1], Yang Song[1], Paul Young[2,3], Daniela Traini[2,3], Lucy Morgan[4],
Hui-Xin Ong[2,3], Lachlan Buddle[4], Dagan Feng[1]

[1]BMIT Research Group, School of IT, University of Sydney, Australia
[2]Woolcock Institute of Medical Research, Australia
[3]School of Medical Sciences, University of Sydney, Australia
[4]Department of Respiratory Medicine, Concord Repatriation General Hospital, Australia

ABSTRACT

Defective mucociliary clearance is inevitably seen in the chronic lung diseases and contributes substantially to their pathologies, and increasing the ciliary motility with external stimuli is considered to be efficient to relieve it. Ciliary Beating Frequency (CBF) is a regulated measurement to evaluate the drugs by comparing their effects on the motility of cilia. Therefore, CBF estimation is crucial for the therapeutic assessment on the defective mucociliary clearance diseases, and digital high speed imaging (DHSI) analysis provides an effective tool to measure CBF. However, the limitations of the current estimation approaches obstruct the accurate description of ciliary motility due to the introduced noise. Therefore, in this study, we propose a new image-based CBF estimation approach, which contains two main stages: a moving ciliated cell alignment is firstly conducted to remove the movement of ciliated cell, and then a threshold-based CBF estimation is designed to record the CBF by observing the beating cilia only. Different from the traditional approaches, the proposed scheme captures the most significant characteristics of the ciliary motility so that it can better describe the responses of the cilia to various drugs.

Index Terms— Mucociliary clearance, beating cilia, cell alignment, CBF estimation

1. INTRODUCTION

Mucociliary clearance plays a major role in clearing mucus by eliminating the harmful debris, *e.g.*, particles and pathogens contained in the air people breath. Ciliary beating is an integral part of the mucociliary transport apparatus, which is stimulated by β-agonists in a variety of mammalian airway epithelial cells [1]. Therefore, increasing the ciliary motility with external stimuli is thought to be an efficient way to assist the defective mucociliary clearance. While orthodox β-agonists, such as salbutamol [2] and isoproterenol [3], have demonstrated their effects in increasing ciliary motility, longer acting drugs have emerged with greater subtype specificity. Hence, examining the effects of recently developed drugs by drawing comparisons with older ones is significant to show whether such drugs are capable of addressing the therapeutic goals of defective mucociliary clearance diseases.

Ciliary Beating Frequency (CBF) is a tightly regulated measurement to describe the ciliary beating properties, and thus is widely used to measure the ciliary motility for the assessment of new drugs. Currently, image-based methods are widely used to estimate CBF with a digital high speed imaging (DHSI) analysis that enables the frame-by-frame observation of ciliary movement. The commonly used approach is applying the Fast Fourier Transform (FFT) on intensity signal, which is temporally extracted from the region of interest (ROI) above the cilia [4, 5]. While such ROI-based methods could capture the differences, the noise introduced from the data acquisition would restrict the reliability of the obtained CBF on describing the ciliary motility. Firstly, cilia are densely packed and wave in a metachronal process [6], therefore the observation sometimes comes from the overlapping cilia. Furthermore, they are close together on the ciliated surface, *e.g.*, cell, thus the cilia are more likely to be obscured, especially when the ciliated cell is beating simultaneously.

Therefore, removing the influences from these issues would be helpful to better describe the changes of the ciliary motility. First of all, the movement of the ciliated cell should be eliminated so as that the extracted intensity signal could only reflect the ciliary beating. A coregistration method was proposed for this aim by rotating all frames [7], which refers to a better CBF estimation. However, this approach highly depends on the cell segmentation to extract the rotation axis. In addition, the selection of ROI could also affect the estimation of CBF [4, 5]. The ROIs are normally selected manually, which would inevitably incorporate more than the desirable beating cilia such as moving ciliated surface and floating debris, and tiny shift would result in the differences since the images record a combination of overlapping cilia [8] even the ROI could precisely locate the cilia.

In light of above, we design a new image-based CBF estimation scheme from another perspective, which contains two main stages: moving cell alignment and threshold-based CBF estimation. While the first stage removes the effect from the movement of ciliated cell, the second tries to describe the most significant characteristics by only observing the beating cilia.

2. METHOD

2.1. Data Acquisition

Samplings of primary ciliated epithelial cells were obtained via nasal brushing from healthy volunteers. This was subsequently suspended in Medium 199 (Sigma, Australia), and mounted onto the stage of a light microscope (Olympus IX70, Japan). The camera (60 frames per second, Nikon D7100, Japan) was connected to the microscope to record the videos. The acquisition for CBF estimation was recorded during the acquisition through a photo-multiplier (Zeiss, West Germany) where the electronic signals from the photometer will be delivered through an oscilloscope and subsequently recorded by Mac-Lab recording system. The acquisition estimation was used as a criterion to evaluate the proposed method.

2.2. Moving Cell Alignment

The cell alignment process is to transform all frames of the video file into the same coordinate system, making the cells located in the same position, so that the movement of cell could be eliminated. It contains two major components: frame-to-frame alignment and overall alignment.

2.2.1. Frame-to-Frame Alignment

Given two frames, *i.e.*, the reference frame Frm_{rf} and the target frame Frm_{tg}, frame-to-frame alignment is to adjust Frm_{tg} according to Frm_{rf} so that the cells in these two frames are matched together. Based on our visual inspection, cells usually move in two manners: translation and rotation. Hence, the cell in Frm_{tg} is translated and/or rotated to its original position in Frm_{rf}.
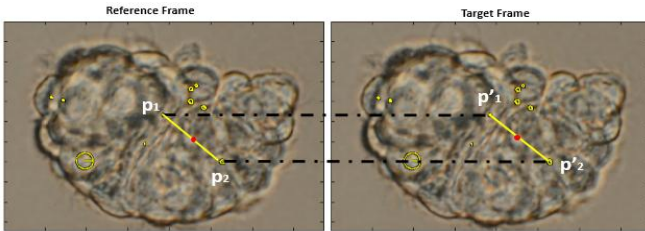

Fig. 1. The illustration of frame-to-frame alignment of sample ciliated cell. The corresponding key points (the yellow circles) in target are firstly selected based on the selected ones in reference (the black dash lines). Then, the target is translated and/or rotated to make the midpoints (the red points) overlapping and the directions of the selected key points (the yellow lines) same.

Specifically, scale-invariant feature transform (SIFT) algorithm is used to detect the key points from both of the frames, and the top matched pairs are selected to determine the alignment. As shown in Fig.1, two key points (p_1, p_2) from Frm_{rf} and the corresponding points (p'_1, p'_2) from Frm_{tg} are firstly selected. SIFT generates one feature vector for each of the key points, and then key point p' is determined if it has the smallest distance, *i.e.*, *L2* norm of the difference with p in terms of the feature vector, denoting as *diff(p, p')*. Following that, Frm_{tg} is translated to make the midpoints of (p'_1, p'_2) and (p_1, p_2) overlapping, and then is rotated to equalize the directions of (p'_1, p'_2) and (p_1, p_2).

The alignment highly depends on the selection of the key point pair; hence, several more pairs are selected to find the optimal one by making the average distance among them smallest after the alignment, as:

$$opt(p_1, p_2) = \min_{(p_1, p_2)} distance(Frm'_{tg}, Frm_{rf}) \qquad (1)$$

$$distance(Frm'_{tg}, Frm_{rf}) = \sum_{i \in [1,K]} diff(p_i, p'_i) / K \qquad (2)$$

where K is the total number of the selected pairs, Frm'_{tg} is the aligned target.

2.2.2. Overall Alignment

Based on the frame-to-frame alignment, the overall alignment is to adjust all frames so that the cell could be immobilized. In our proposed method, each frame is adjusted locally, *i.e.*, the target is aligned according to its former neighbouring frames that have already been adjusted.

Specifically, for each target frame Frm_{tg} in the whole frame set $FS=\{Frm(f); f=1 \dots F\}$, frame-to-frame alignment is conducted individually with each of the references, called reference set $RS(Frm_{tg})=\{Frm_{rs}(r): r=1 \dots R\}$ that are the former neighbouring R frames of Frm_{tg}. The effect of the individual alignment is evaluated through calculating the distance between the aligned target Frm'_{tg} and the whole $RS(Frm_{tg})$, as:

$$distance(Frm'_{tg}, RS) = \sum_r distance(Frm'_{tg}, Frm_{rs}(r)) / R \quad (3)$$

The benefits of incorporating several reference frames locally are twofold: firstly, as the time goes on, the latter frame might deviate from the former one to a larger extent, which makes it hard to match them if a global benchmark frame is fixed for all frames, *e.g.*, the first one; secondly, the alignment deviation of the target might be magnified if only one neighbouring reference is involved.

Adjusting the target according to the alignment that makes $distance(Frm'_{tg}, RS)$ minimum is likely to be feasible; however, through the inspections on the experiment results, we found the minimum was more likely to be achieved with the nearest reference frame, especially when this frame was not moved in its own process. Therefore, each of the alignments is accepted with the probability to incorporate the effects from the relatively distant references:

$$p = \begin{cases} 1 & if \ C(r) < C_{min} \\ \exp(-\dfrac{C(r) - C_{min}}{sqrt(C_{min}) \cdot T}) & if \ C(r) \geq C_{min} \end{cases} \quad (4)$$

$$C(r) = distance(Frm'_{tg}(r), RS) \quad (5)$$

where $C(r)$ is the cost of current alignment in terms of the distance between the adjusted target and the $RS(Frm_{tg})$, C_{min} is the current minimum cost among the former alignments, and T is a user-set variable to regularize the probability.

```
Inputs: FS, R, K, T(1), c, I.
Outputs: AFS
Steps:
    for Frm_tg in FS
        for Frm_fr in RS(Frm_tg)
            for it in 2…I
                T(it) := T(it-1) - c
                Frm'_tg := f2f_align(Frm_tg, Frm_fr, K)
                p := prob( Frm'_tg, T(it))
                if p > rand(0,1)
                    Frm_tg := Frm'_tg
        add(AFS, Frm_tg)
    end for
    return: AFS
```

Fig. 2. The procedure of overall alignment: *f2f_align* is the frame-to-frame alignment of Frm_{tg} according to Frm_{fr} with the K point pairs; *prob* returns the accept probability p based on Eq.(4); *rand* generates a uniform random number between 0 and 1; *add* puts the aligned target into the result *AFS*. In our experiments, R and K were set as 3 and 10 respectively, and T was initialized with 100, updated within $I = 8$ iterations with $c = 10$.

To further refine the alignment, variable T is used to adjust the aligned target iteratively. By starting at a high T and constantly decreasing T, a more optimal alignment would be obtained, which is closer to the reference set overall. In particular, the decreasing T in E.q. (4) would generate smaller accept probabilities, and gradually lead to the deep minimum of the cost. T is decreased with the following scheme:

$$T(it) = T(it - 1) - c \quad (6)$$

where it is the index of the total I iteration, and c is a constant.

The final result of overall alignment $AFS=\{Frm'(f): f=1…F\}$ is obtained by replacing the original frame with the aligned frame. The procedure of the overall alignment is shown in Fig. 2.

2.3. CBF estimation

Once the cell alignment has been conducted, CBF is going to be measured. To handle the limitations of ROI-based approaches, we perform the estimation by selecting a threshold within the whole field frequency [9], and then computing average (± standard deviation) [10] of the over-threshold frequencies as the CBF estimation, shown in Fig.3.

Specifically, the whole field analysis is firstly used to obtain the frequency map (as shown in Fig.3 (b)), which

indicates the frequency of each pixel. Then, instead of selecting the ROI and frequency range manually, a threshold is extracted from the frequency distribution by extracting the breaking point (as shown in Fig.3 (d)).

As for the proposed approach, on the one hand, eliminating the lower frequencies could highlight the beating cilia due to the fact that the beating frequencies of floating debris [9] and moving cells [7] are lower than the beating cilia. On the other hand, it could reduce the influence from the overlapping cilia that usually present lower frequencies.
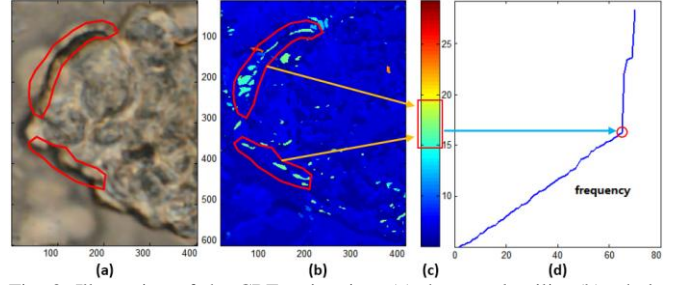

Fig. 3. Illustration of the CBF estimation: (a) the sample cilia, (b) whole field frequency map, (c) the frequency color bar, (d) the frequency distribution. The beating cilia (red circles in (a) and (b)) are extracted by eliminating the regions (blue areas in (b)) with the frequencies below the breading point (red circle in (d)), and the average frequency ± standard deviation (red rectangle in (c)) is calculated as the CBF estimation.

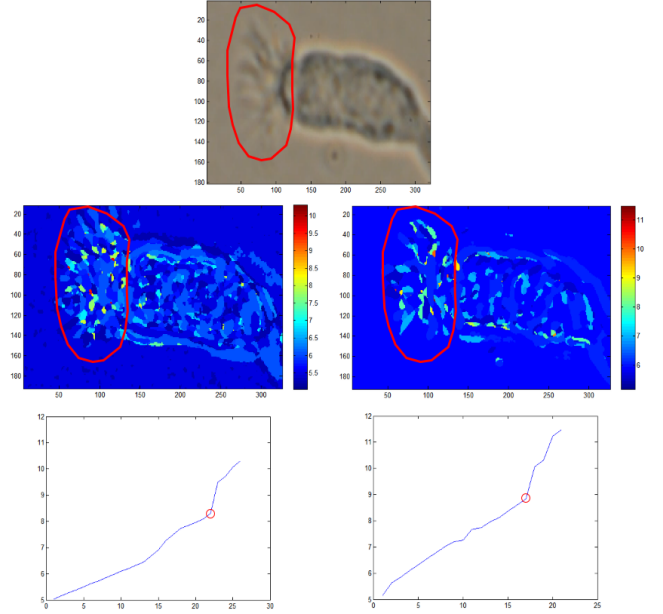## 3. EXPERIMENTS AND RESULTS

Fig. 4. Results of the proposed method on the cilia video. The top diagram is a single frame extracted from the video, indicating the cilia (circled in red) and ciliated cell. The remaining diagrams show the whole field frequency map and the frequency distribution respectively.

Fig. 4 shows the results of the proposed method on the cilia beating video, and the corresponding statistics about the CBF estimation are given in Table I. Firstly, we observe that the threshold (8.31Hz) in threshold-only approach is within the average acquisition CBF estimation (7.36 ± 1.55Hz), and

the maximum frequencies of both the two approaches are all around 10Hz, suggesting that the proposed threshold-based estimation could describe the ciliary motility properly in terms of the acquisition estimation. Secondly, the comparison between the two whole field frequency maps in Fig.4 shows the frequencies of cell region in with-alignment approach are relatively lower regarding to the surrounding regions, indicating that the movement of the cell can be effectively removed by the proposed moving cell alignment.
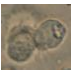
TABLE I
DETAILED STATISTICS OF FIG.4

CBF(Hz)	Threshold	Avg	SD	Max
Acqu	7.36		1.55	10.00
Thd-only	8.31	9.47	0.28	10.30
Alg+Thres	8.83	**9.72**	**0.64**	11.47

Acqu: acquisition estimation; Thd-only: threshold-based without alignment; Alg+Thres: threshold-based with alignment

The final CBF estimation of this case is set as 9.72±0.64Hz through our proposed scheme. The advantages of such estimation are two-fold. Firstly, the threshold-based estimation eliminates the noise frequencies introduced by the ROI selection, therefore the average CBF is increased to 9.47Hz from 7.36Hz since the noisy frequencies are usually from the debris and cell that move less intensely. Secondly, the alignment removes the movement of the cell, leading to a 0.5Hz increment of threshold over threshold-only approach due to the fact that the moving cell shifts the cilia remotely so that it takes a longer time for the cilia to return their original positions.

TABLE II
CBF ESTIMATION UPON THREE CASES WITH VARIOUS CELL MOVEMENTS

Case	Approach	Threshold	Avg	SD	Max
Still	Acqu	10.56		1.34	15
	Thd-only	11.12	11.87	0.99	16.5
	Alg+Thres	11.23	**12.03**	**0.56**	14.04
Media	Acqu	7.45		1.48	12
	Thd-only	8.66	9.10	1.71	12.29
	Alg+Thres	9.13	**11.4**	**0.78**	12.64
Intense	Acqu	9.95		1.66	15
	Thd-only	10.65	12.81	3.17	18.26
	Alg+Thres	10.53	**15.09**	**2.06**	22.4

The statistics of another three cases is reported in Table II to illustrate the performance of the proposed method upon various conditions. In particular, the cases were selected based on the movement of cells through our visual inspections, *i.e.*, still, medium, and intense respectively. While the threshold-only approach makes reasonable estimation regarding to the acquisition estimation and obtains the increments evenly in all of the three cases (1.31Hz, 1.65Hz and 2.86Hz respectively), CBFs are changed to various extents when the alignment is

incorporated responding to the various movements of the cells (1.47Hz, 3.95Hz and 5.14Hz respectively).

Totally, the proposed CBF estimation scheme aims at describing the ciliary beating with the most significant characteristics by eliminating the undesirable noises from the moving cell, overlapping cilia, *etc.*, thus it could better capture the changes of ciliary motility over the acquisition estimation. This would be more suitable for the aim of therapeutic assessments on defective mucociliary clearance diseases that require the comparisons according to whether the drugs do promote the ciliary beating so that they can accelerate the mucociliary transport. More clinical studies will be conducted to further investigate the practicability of the proposed CBF estimation.

4. CONCLUSIONS AND FUTURE WORKS

In this study, we propose a new design of image-based CBF estimation to assist the evaluation of new drugs in increasing ciliary motility. Firstly, a moving cell alignment is conducted to eliminate the influence of movement of cell. The target frame is aligned locally according to several of its former neighbouring frames, reaching the overall balanced position. Then, a threshold-based CBF estimation is proposed to extract the beating cilia to eliminate the influence from overlapping cilia, *etc.* The proposed scheme could better describe the motility of cilia to evaluate the effects from various defective mucociliary clearance drugs.

5. REFERENCES

[1] M. Salathe, "Effects of β-agonists on airway epithelial cells," *Journal of allergy and clinical immunology,* vol. 110, pp. 275-281, 2002.

[2] J. Devalia, et al., "The effects of salmeterol and salbutamol on ciliary beat frequency of cultured human bronchial epithelial cells, in vitro," *Pulmonary pharmacology,* vol. 5, pp. 257-263, 1992.

[3] S. Yanaura, N. Imamura, and M. Misawa, "Effects of beta-adrenoceptor stimulants on the canine tracheal ciliated cells," *Japanese journal of pharmacology,* vol. 31, pp. 951-956, 1981.

[4] M. Salathe and R. J. Bookman, "Mode of Ca2+ action on ciliary beat frequency in single ovine airway epithelial cells," *The Journal of Physiology,* vol. 520, pp. 851-865, 1999.

[5] L. Zhang, et al., "Oscillations in ciliary beat frequency and intracellular calcium concentration in rabbit tracheal epithelial cells induced by ATP," *The Journal of Physiology,* vol. 546, pp. 733-749, 2003.

[6] Y. Won-Jin, *et al.*, "Directional disorder of ciliary metachronal waves using two-dimensional correlation map," *IEEE Trans. Biomedical Engineering,* vol. 49, pp. 269-273, 2002.

[7] E. Parrilla, et al., "Optical flow method in phase-contrast microscopy images for the diagnosis of primary ciliary dyskinesia through measurement of ciliary beat frequency. Preliminary results," in *ISBI*, 2012, pp. 1655-1658.

[8] M.A. Chilvers, et al., "Analysis of ciliary beat pattern and beat frequency using digital high speed imaging:comparison with the photomultiplier and photodiode methods," *Thorax*, vol. 55, pp. 314-317, 2000.

[9] J. H. Sisson, J. A. Stoner, B. A. Ammons, and T. A. Wyatt, "All-digital image capture and whole-field analysis of ciliary beat frequency," *Journal of Microscopy,* vol. 211, pp. 103-111, 2003.

[10] M. A. Chilvers, et al., "Ciliary beat pattern is associated with specific ultrastructural defects in primary ciliary dyskinesia," *Journal of Allergy and Clinical Immunology,* vol. 112, pp. 518-524, 2003.